

Solution Structural Dynamics of HIV-1 Reverse Transcriptase Heterodimer[†]

James M. Seckler,[‡] Kathryn J. Howard,[§] Mary D. Barkley,^{*,‡,§} and Patrick L. Wintrode^{*,‡}

[‡]*Department of Physiology and Biophysics, School of Medicine, and* [§]*Department of Chemistry, Case Western Reserve University, 10900 Euclid Avenue, Cleveland, Ohio 44106*

Received May 7, 2009; Revised Manuscript Received July 13, 2009

ABSTRACT: Crystal structures and simulations suggest that conformational changes are critical for the function of HIV-1 reverse transcriptase. The enzyme is an asymmetric heterodimer of two subunits, p66 and p51. The two subunits have the same N-terminal sequence, with the p51 subunit lacking the C-terminal RNase H domain. We used hydrogen exchange mass spectrometry to probe the structural dynamics of RT. H/D exchange revealed that the fingers and palm subdomains of both subunits form the stable core of the heterodimer. In the crystal structure, the tertiary fold of the p51 subunit is more compact than that of the polymerase domain of the p66 subunit, yet both subunits show similar flexibility. The p66 subunit contains the polymerase and RNase H catalytic sites. H/D exchange indicated that the RNase H domain of p66 is very flexible. The β -sheet β 12- β 13- β 14 lies at the base of the thumb subdomain of p66 and contains highly conserved residues involved in template/primer binding and NNRTI binding. Using the unique ability of hydrogen exchange mass spectrometry to resolve slowly interconverting species, we found that β -sheet β 12- β 13- β 14 undergoes slow cooperative unfolding with a $t_{1/2}$ of <20 s. The H/D exchange results are discussed in relation to existing structural, simulation, and sequence information.

Reverse transcriptase performs the first step in replication of HIV.¹ RT copies the single-stranded viral RNA genome into a double-stranded proviral DNA prior to insertion by integrase into a chromosome of the infected cell (*1*). RT has RNA- and DNA-dependent DNA polymerase activities and RNase H activity. The mature enzyme is a heterodimer of p66 and p51 subunits; p51 has the same N-terminal polymerase domain as p66 but lacks the C-terminal RNase H domain. The enzyme has an asymmetric structure (*2*). The p66 subunit contains the enzyme active sites (*3*), whereas the p51 subunit appears to have a structural function. The p66 polymerase domain has a right-handed conformation like other polymerases with fingers (residues 1–85, 118–155), palm (residues 86–117, 156–236), and thumb (residues 237–318) subdomains plus a connection subdomain (residues 319–426). The fingers, palm, and thumb subdomains of p66 form the template/primer binding cleft with the polymerase active site residues (D110, D185, and D186) in the palm subdomain (*4*). Although the four subdomains of the polymerase domain have similar folds in p66 and p51, their relative orientations differ in the two subunits (Figure 1).

Numerous crystal structures are available for wild-type and mutant HIV-1 RTs in the absence and presence of various substrates and inhibitors. The conformation of the p51 subunit is essentially the same in all of the structures, whereas the p66

polymerase domain adopts both open and closed positions of the fingers and thumb subdomains, suggesting that RT is quite flexible. The crystallographic *B*-factors of two unliganded wild-type RT structures (same space group) identify the same mobile regions in the p51 subunit but somewhat different mobile regions in the p66 subunit (*5, 6*). In addition to structural evidence, computational studies have explored the flexibility of RT and its complexes and proposed possible functional roles for protein dynamics in translocation of template/primer substrate (*7–10*), inhibition by NRTIs (*11*) and NNRTIs (*7, 9, 10, 12–14*), and drug resistance (*13*). However, experimental studies of RT conformation and dynamics in solution are few. Both open and closed conformations of the p66 polymerase domain were observed by site-directed spin labeling (*15*), and the solution structure and backbone dynamics of the isolated RNase H domain were determined by NMR (*16–18*).

This paper uses hydrogen exchange mass spectrometry to examine the solution conformation and dynamics of HIV-1 RT. HXMS studies provide a medium resolution snapshot of the exchange of amide protons on the peptide backbone (*19*). The H/D exchange was monitored as a function of time after dilution of the RT heterodimer into deuterated buffer. The rate of exchange in each peptide depends on the extent and lability of hydrogen-bonded secondary structures and on solvent accessibility. Exchange rates were measured separately for p66 and p51 subunits of the heterodimer, mapped onto the amino acid sequences, and compared to crystallographic and computational results. The implications of the protein dynamics for RT function are discussed.

EXPERIMENTAL PROCEDURES

Protein Preparation. Biochemical reagents and chemicals were obtained from Roche Applied Science (Indianapolis, IN) and Sigma Chemicals (St. Louis, MO) unless otherwise specified.

[†]This work was supported by NIH Grant GM071267 (M.D.B.) and Case/UHC Center for AIDS Research Grant AI36219 (P.L.W.).

^{*}To whom correspondence should be addressed. M.D.B.: e-mail, mdb4@case.edu; phone, 216-368-3178; fax, 216-368-3952. P.L.W.: e-mail, patrick.wintrode@case.edu; phone, 216-368-3178; fax, 216-368-3952.

Abbreviations: ANM, anisotropic network model; EDTA, ethylenediaminetetraacetic acid; GNM, Gaussian network model; HIV-1, human immunodeficiency virus type 1; HXMS, hydrogen exchange mass spectrometry; NNRTI, nonnucleoside reverse transcriptase inhibitor; NRTI, nucleoside reverse transcriptase inhibitor; RT, reverse transcriptase; Tris, tris(hydroxymethyl)aminomethane.

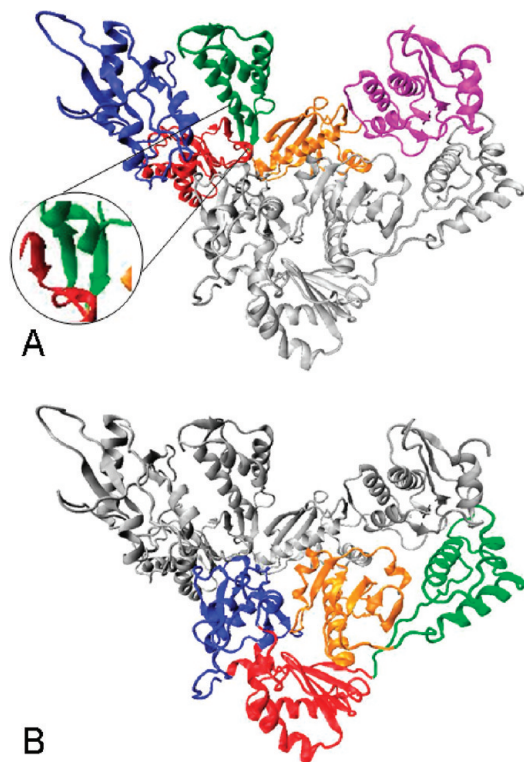


FIGURE 1: Structure of unliganded HIV-1 RT. (A) p66 subunit (colored) and p51 subunit (gray) and (B) p66 subunit (gray) and p51 subunit (colored). Four subdomains of the polymerase domain, fingers (blue), palm (red), thumb (green), and connection (orange), and RNase H domain (magenta). Protein Data Bank ID 1DLO (5).

RT buffer D is 0.05 M Tris (RNase, DNase-free, pH 7.2), 25 mM NaCl, 1 mM EDTA, and 10% (v/v) glycerol (molecular biology grade redistilled). PBS is 0.1 M phosphate buffer (pH 7.2) and 0.15 M NaCl (Pierce, Rockford, IL). D₂O was purchased from Cambridge Isotope Laboratories (Andover, MA). HIV-1 RT subunits with N-terminal hexahistidine extensions were expressed separately in *Escherichia coli* M15 strains carrying pDM1.1 plasmids p6H RT for p66 and p6H RT51 for p51. Cells were cultured at 37 °C to an optical density of 0.7 at 600 nm, induced with 200 μ g/mL isopropyl β -D-1-thiogalactoside, grown for 3 h, and harvested. RT proteins were purified as described (20) and modified (21).

The N-termini of p66 and p51 were labeled with biotin using the EZ-Link NHS-PEO₄ biotinylation kit (Pierce, Rockford, IL). Protein samples were dialyzed overnight against 2 \times 1 L of PBS, incubated overnight on a rocker with 10-fold molar excess of biotin, and then dialyzed against RT buffer D containing 50% glycerol at 4 °C. Labeling was confirmed to be 100% by the HABA avidin assay provided with the kit, SDS-PAGE mobility shift, and mass spectrometry. The p66/p51 heterodimer with one biotin-labeled subunit was prepared by incubating equimolar mixtures of labeled and unlabeled subunits in RT buffer D containing 50% glycerol for at least 5 days. Activity of biotin-labeled p66/p51 was confirmed using the EnzCheck reverse transcriptase assay kit (Invitrogen Corp., Carlsbad, CA). Total protein concentrations of p66/p51 solutions are 20–30 μ M (monomer units). Based on the dimerization constants (21), the p66/p51 solutions contain >84–87% heterodimer.²

²Estimated using K_d values determined in RT buffer D at 5 °C. Preliminary data indicate that increasing glycerol concentration favors dimerization.

Peptide Mapping by HPLC-Tandem Mass Spectrometry. Peptide mapping experiments were carried out as described previously (22) with the following modification. Five μ g (0.08 nmol) of p66 in 5 μ L of RT buffer D was mixed with 500 μ L of 100 mM NaH₂PO₄ (pH 2.4) and was digested with 5 μ L of 1 mg/mL porcine pepsin in H₂O. Sequencing by tandem mass spectrometry was carried out using an LCQ-DECA quadrupole ion trap mass spectrometer (ThermoElectron). Additional peptide mapping experiments were conducted on an LTQ-FT ion cyclotron resonance mass spectrometer (ThermoElectron) in order to confirm peptide identification by exact mass.

H/D Exchange of the p66/p51 Heterodimer. RT heterodimer with either the p66 or p51 subunit containing an N-terminal biotin tag (11.2 μ g of labeled p66 or 9.0 μ g of labeled p51) in RT buffer D–H₂O containing 50% glycerol was diluted 10-fold into RT buffer D–D₂O (pD 7.2) containing 5% glycerol and incubated for different times from 5 s to 2 h at 25 °C. Exchange was quenched by diluting the protein sample 5-fold with 100 mM NaH₂PO₄ (pH 2.4) at 4 °C. RT is reversibly denatured by acidic pH (23), and the biotin-labeled subunit was removed using a streptavidin column or beads. For column separations, the protein sample was loaded onto a 1 mL HiTrap streptavidin HP column (GE Healthcare Bio-Sciences, Piscataway, NJ), and the column was washed with 1 mL of 100 mM NaH₂PO₄ (pH 2.4). The biotin-labeled subunit was bound to the column; the unlabeled subunit was collected in the flow-through. The column was then washed with 20 mL of 100 mM NaH₂PO₄ (pH 2.4) to remove any residual free subunit prior to reuse. SDS gel electrophoresis showed a single band corresponding to the unlabeled subunit. For bead separations, the protein sample was mixed with 20 μ L of Ultralink immobilized neutraavidin protein beads (Pierce, Rockford, IL) and vortexed for 30 s. The mixture was then centrifuged for 30 s, and the supernatant was collected. SDS gel electrophoresis showed that ~85% of the labeled subunit was removed (Supporting Information Figure S1). The amount of residual unlabeled subunit estimated from the mass spectra is ~15%. Comparison of mass spectra of identical peptides obtained from samples separated on columns versus beads showed that a 15% background signal did not compromise our ability to quantify deuterium uptake. The signal from the residual labeled subunit shifts the centroid mass by ≤ 0.1 Da.

Isotope Analysis by HPLC-ESI Mass Spectrometry. The deuterium-labeled protein was digested on ice with 5 μ L of 1 mg/mL porcine pepsin in H₂O for 5 min and analyzed by HPLC-MS as described elsewhere (24). Deuterium levels for each peptide were corrected for back-exchange using the equation

$$D = \frac{m - m0\%}{m100\% - m0\%} \times N \quad (1)$$

where D is the number of amide hydrogens exchanged with deuterium, m is the centroid mass of the peptide at a given time point, $m0\%$ is the mass of the undeuterated peptide, $m100\%$ is the mass of the fully deuterated peptide, and N is the number of amide hydrogens in the peptide. D is then plotted versus time, and the resulting curve is fitted to a triple exponential function using nonlinear least squares (OriginLab).

$$D = N - N_{\text{fast}}e^{-k_{\text{fast}}t} - N_{\text{medium}}e^{-k_{\text{medium}}t} - N_{\text{slow}}e^{-k_{\text{slow}}t} \quad (2)$$

where N_{fast} , N_{medium} , and N_{slow} are the number of fast, medium, and slow exchanging amide hydrogens in the peptide and k_{fast} ,

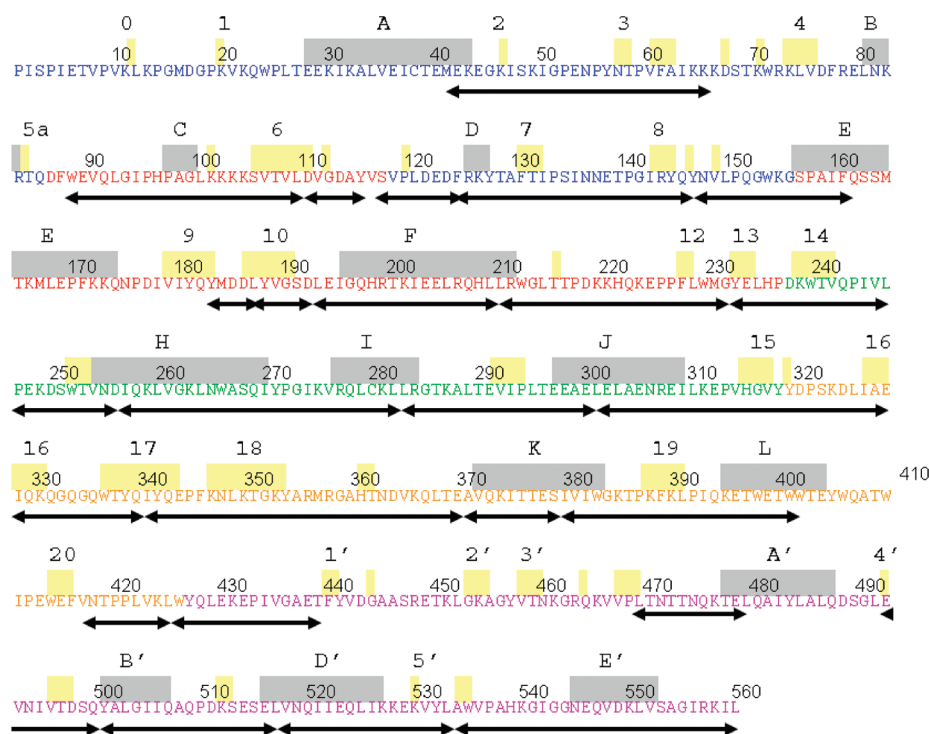


FIGURE 2: Peptides used for analysis of H/D exchange data. Peptides are indicated by double-headed arrows under the sequence of HIV-1 p66. Color of amino acid sequence indicates polymerase subdomains, fingers (blue), palm (red), thumb (green), and connection (orange), and RNase H domain (magenta). Structural elements from 1DLO: α -helices (gray bars), letters; β -strands (yellow bars), numbers. The secondary structural elements are author's choice as identified in the Protein Data Bank.

k_{medium} , and k_{slow} are the rate constants of the observed exchange.

RESULTS

Peptide Mapping and Identification. A total of 50 peptic fragments were identified by tandem mass spectrometry giving a total sequence coverage of 75% for the p66 subunit and 77% for the p51 subunit. The longest of these peptic fragments has 30 exchangeable amide hydrogen atoms and the shortest has five, with an average among all of the peptides of 15 exchangeable amide hydrogens; 27 fragments were analyzed in HXMS experiments. These are well distributed throughout the entire protein sequence (Figure 2). The remaining 23 peptic fragments provide largely redundant information; different peptides with substantial sequence overlap show similar exchange behavior. The analyzed peptic fragments cover 63% of the amino acids in the dimer interface of the p66 subunit and 87% of the interface residues of the p51 subunit (21). The sequence coverage of residues involved in template/primer binding is 85% of the total DNA/DNA and RNA/DNA contacts made by both subunits, including the catalytic triad in the polymerase active site, four of the six residues which make contact with dTTP substrate, and three of the four conserved residues in the RNase H active site (25, 26). The sequence coverage of the hydrophobic NNRTI binding pocket is 83% (27).

Kinetics of H/D Exchange. Figure 3A shows raw mass spectra of the peptide from residues 257–282 of RT incubated for different times in deuterated buffer. The shift in mass as deuteriums replace hydrogens along the amide backbone is easily seen. These spectra were used to make a plot of deuterium uptake vs time. The solid line shows a good fit of these data to eq 2 (Figure 3B). Rate constants obtained from curve fitting to the analyzed peptides for p66 and p51 are given in Supporting

Information Tables S1 and S2. The rate constants of fast exchanging hydrogens give exchange half-lives on the order of seconds, which is comparable to the values expected for completely unprotected hydrogens (28). Thus the fast exchanging hydrogens are most likely exposed to solvent and not involved in hydrogen bonding. The rate constants for medium exchanging hydrogens give half-lives on the order of 1–10 min, and these hydrogens are likely in structured regions that undergo substantial conformational fluctuations. Slow hydrogens exchange with half-lives on the order of 1–100 h and are therefore located in regions of highly stable structure in solution. It was not possible to fit all peptide exchange curves to eq 2 with high confidence. In some cases, this was because the deuterium level showed a rapid rise at early labeling times followed by a very abrupt leveling off. In other cases, the slow rate constant was indeterminate due to extremely stable secondary structure. However, in both of these cases, the number of slow exchanging hydrogens could be determined from the number of hydrogens that remained unexchanged at the longest incubation times. Rate constants, of course, could not be determined for these, only the fact that they exchange considerably more slowly than the fast or medium hydrogens.

Percent exchange at various incubation times is mapped onto the sequence of the p66 subunit of RT in Figure 4A. The fingers and palm subdomains have stable secondary structure, as evidenced by the slow rates of H/D exchange. The most notable exception is the peptide spanning residues 210–231, which shows little protection from exchange. Peptide 88–109 shows considerable protection at the earliest labeling times but shows moderate levels of exchange at later times. The catalytic triad and dNTP binding site are both wholly contained within the fingers and palm subdomains (25). The catalytic triad is encompassed by two small peptides, one of which (183–187) remains almost

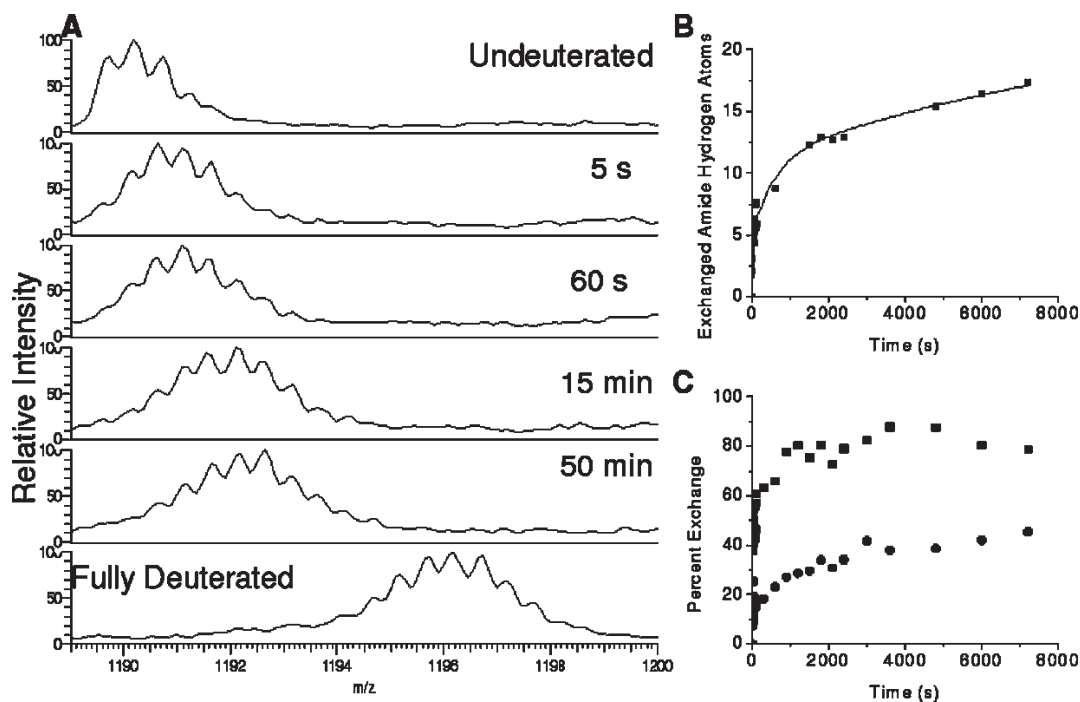


FIGURE 3: HXMS data and curve fitting of H/D exchange data for the p66 subunit. (A) Raw spectra showing a peak for peptide 41–61 at different incubation times in RT buffer D–D₂O. Spectra of undeuterated and fully deuterated reference samples also shown. (B) Number of amide hydrogens exchanged with deuterium vs time for peptide 257–282. Solid line is fit of the data to eq 2. (C) Percent exchange vs time of two peptides. Peptide 147–160 (lower curve) is in a buried region of the fingers/palm subdomains in the crystal structure of HIV-1 RT (1DLO). Peptide 283–300 (upper curve) is in a surface-exposed region of the thumb subdomain.

completely protected from exchange for the duration of the time course, while the other (110–115) is reasonably stable but does show exchange. Three of the six residues in the dNTP binding site are part of the short peptide (110–115) that contains a single residue from the catalytic triad. The fourth dNTP binding residue is contained in a third peptide (147–160) that also shows a low rate of exchange (Figure 3C, lower curve). This indicates that both the polymerase active site and the dNTP binding site are structured and stable.

The NNRTI binding pocket exists only in structures of RT–NNRTI complexes. It includes two β -sheets that are also present in structures in the absence of drug. The first of these sheets, β 6– β 10– β 9, is covered by four different peptides (88–109, 110–115, 183–187, 187–192). Exchange rates in these peptides show that β 10 and β 9 are extremely stable, while β 6 is folded but flexible. In contrast, the second sheet, β 12– β 13– β 14, is covered by two peptides (210–231, 232–246), which both show extremely high rates of exchange. As discussed below, the peptide covering β 13– β 14 (232–246) undergoes slow cooperative unfolding. All peptides within the thumb subdomain show low levels of exchange at early labeling times but moderate to high levels of exchange at later labeling times, suggesting that the entire subdomain is structured but flexible. Rates of H/D exchange in the connection subdomain are faster on average than in the fingers, palm, and thumb subdomains (except residues 210–246) but are consistent with stable secondary structure. Of the five peptides covering the RNase H domain, only one (492–500) shows a high degree of protection against exchange. This indicates that the RNase H domain is highly flexible. Three of the RNase H catalytic residues (E478, D496, and D549) are covered by three different peptides (469–479, 492–500, 534–560). Two of these three peptides (469–479, 534–560) show high rates of exchange. Some active site residues in both the polymerase and RNase H domains coordinate magnesium ions. Note that the

buffers used in the experiments reported here do not contain magnesium.

The percent exchange at various incubation times for the p51 subunit is given in Figure 4B. Although the tertiary structures of p51 and the p66 polymerase domain differ, the secondary structures are largely identical, and this is reflected in similar H/D exchange rates, albeit with some local differences. The degree of exchange at short labeling times (5–10 s) reflects primarily solvent exposure and hydrogen bonding, and the levels of exchange at 5 s are nearly identical in p66 and p51, consistent with the fact that they possess similar secondary structure. Local differences are seen at longer labeling times, indicating that local flexibility differs between the two subunits. The long stretch of residues from 210 to 246 in the palm and a portion of the thumb are somewhat more flexible in p51, while residues 340–370 in the connection are slightly more rigid. Interestingly, p51 does not show slower exchange overall than p66, indicating that, despite being more compact, p51 is not significantly more rigid than p66.

The dimer interface includes residues from both subunits of the heterodimer. All peptides in the p66 polymerase domain that contain a significant portion of the dimer interface show very slow exchange at the earliest time points, indicating that they are shielded from solvent. This implies that the dimer interface observed in crystals is stable and present in solution. The loop (426–439) that links the connection subdomain to the RNase H domain shows a much greater degree of initial protection than expected for a solvent-exposed loop, consistent with being part of the dimer interface. Because the loop has no secondary structure, the initial protection from exchange is due completely to residues in the dimer interface. However, this peptide exchanges rapidly, indicating that the dimer interface provides little long-term protection from solvent. Four peptides in the RNase H domain also cover residues in the dimer interface. One of these (492–500) shows almost complete protection, and another (501–517) shows

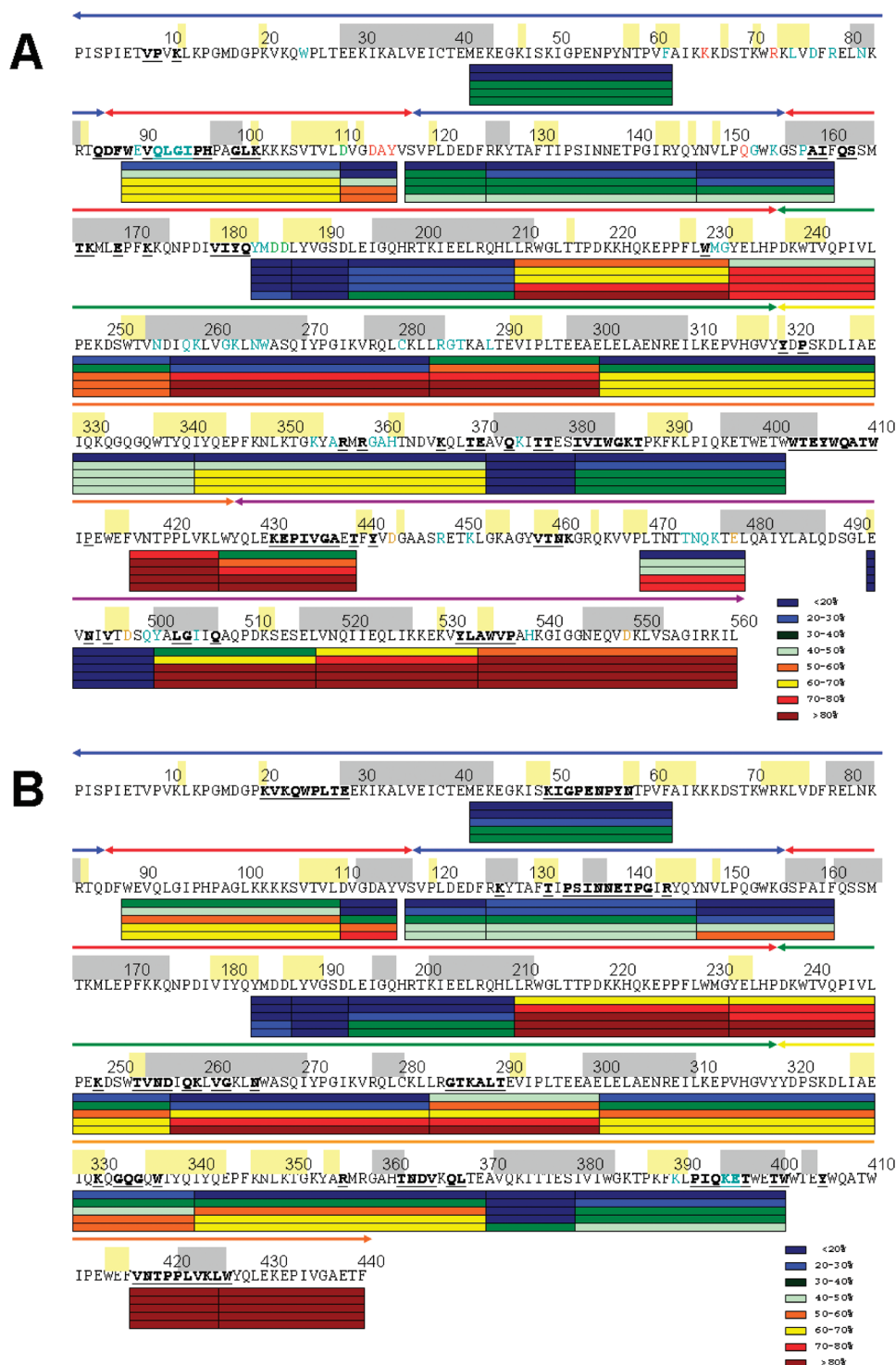


FIGURE 4: Percent exchange of peptides from the (A) p66 subunit and (B) p51 subunit of HIV-1 RT. Colored bars below sequence from top to bottom give exchange at 5, 60, 600, 3000, and 7200 s. Gray and yellow bars above sequence correspond to α -helices and β -sheets. Colored arrows above structural elements indicate polymerase subdomains, fingers (blue), palm (red), thumb (green), and connection (orange), and RNase H domain (magenta). Contact residues: dimer interface (underlined bold face), template/primer substrate binding site (blue), dTTP substrate binding site (red), polymerase active site (green), and RNase H active site (brown).

some initial protection. In the crystal structure, peptide 492–500 is a solvent-inaccessible β -strand, while peptide 501–517 comprises a surface-exposed helix and loop. The other two peptides (518–533, 534–560) show very little initial protection, suggesting that this region of the dimer interface is more labile.

The peptides in p51 that contain portions of the dimer interface likewise show low levels of initial exchange, with two notable exceptions (283–300, 417–425). Interface residues in both of

these peptides make contacts with the RNase H domain of p66; p51 residues 288–290 contact p66 residues 435–439, while p51 residues 417–425 form contacts with p66 residues 503–504 and 532–537. The relative lack of protection in these regions even at short labeling times further supports the conclusion that the dimer interface formed between the RNase H domain and p51 is highly dynamic. Of residues contained in the two unprotected peptides (417–425, 426–440) at the C-terminus of p51, only

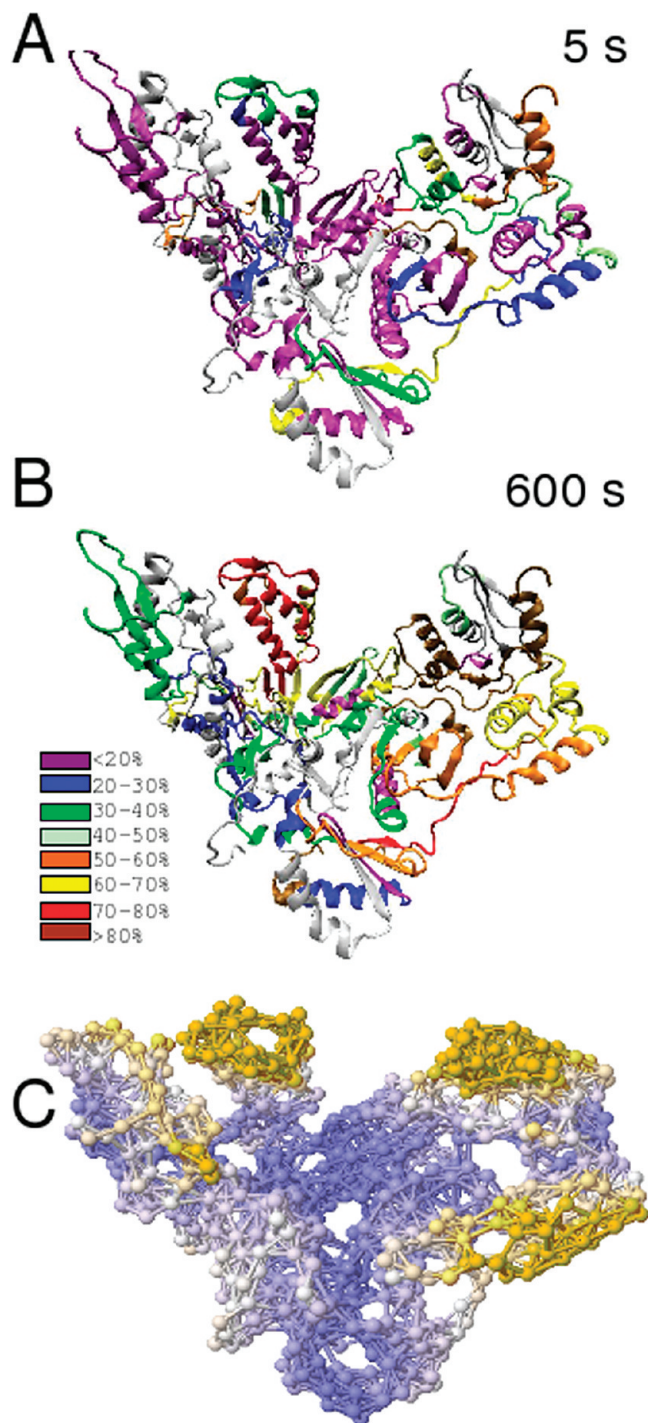


FIGURE 5: Percent exchange for both subunits mapped onto the structure of HIV-1 RT. (A) 5 s and (B) 600 s incubation in RT buffer D-D₂O. Lower percentages correspond to a greater degree of protection from exchange. (C) Mobility in the second mode as calculated by ANM (36). Gold regions represent highly mobile regions; blue regions represent rigid regions.

residues 415–421 appear to be essential for heterodimer formation, although C-terminal truncation of p51 after residue 421 or 426 affects enzyme activity (29).

Figure 5 presents the percent exchange for two time points (5 and 600 s) mapped onto the crystal structure of unliganded HIV-1 RT (5). At 5 s the whole protein shows a great degree of protection from exchange (Figure 5A). By 600 s the fingers and palm subdomains of both subunits form a stable core of the protein that is largely protected from deuterium exchange, while

the rest of the protein appears to be much more flexible, allowing its amide hydrogens to exchange with solvent (Figure 5B).

Comparison to Crystal Structure. Coloring the structure by percent exchange as in Figure 5 has the advantage of presenting the data without making assumptions about the solution structure of the protein. Because of limited resolution, a given peptide may contain secondary structural elements as well as coil regions, skewing the results so that a region with stable secondary structure may appear to be unstructured. This problem is avoided by comparing the number of slow exchanging amide hydrogens from Supporting Information Tables S1 and S2 with the number of hydrogen-bonded amide hydrogens predicted from the crystallographic model of RT using the program WhatIf (5, 30). The ratio of slow exchanging to hydrogen-bonded amide hydrogens serves as a measure of protein flexibility. Table 1 lists the flexibility ratios for each of the analyzed peptides. In cases where the ratio is greater than 1, the additional protection can be explained by solvent shielding. These ratios were used to color the structure of RT (Figure 6). It appears that the stable core formed by the fingers and palm subdomains of both subunits is quite rigid, while the regions adjacent to this core (thumb subdomain of p66 and connection subdomains of both subunits) are more flexible but still stable. The regions distant from the core (RNase H domain of p66 and portions of connection and thumb subdomains of p51) are unstable. Exceptions to this are peptides 210–231, 232–246, and 283–300 (Figure 3C, upper curve) in the p66 subunit and peptide 232–246 in the p51 subunit. All of these regions are much more flexible than would be expected if the secondary structures shown in the crystal structure were stable. It is worth noting that a significant difference in secondary structure between the p66 and p51 subunits is that residues corresponding to β -strands 12 and 14 in p66 do not form β -strands in p51. Instead, they are either missing electron density (strand 12) or adopt a coiled conformation (strand 14).

Slow Cooperative Unfolding/Refolding at the Base of the p66 Thumb Domain. A particular strength of HXMS is its ability to monitor cooperative conformational changes by directly resolving distinct structural populations in solution. If a protein or protein region exists in two distinct, slowly interconverting conformations, then exchange can occur via the EX1 mechanism. The resulting spectrum of the deuterium-labeled sample will exhibit a two-peak pattern or “double isotopic envelope”, with each peak representing one of the conformations (31). In the case of protein unfolding, a lower and higher m/z envelope will correspond to the folded and unfolded forms, respectively. If the protein or region undergoes cooperative unfolding, the lower m/z peak will disappear during continuous incubation in D₂O, while the higher m/z peak will grow, and the rate of the disappearance of the lower peak will provide a measure of the rate of cooperative unfolding. This will be observed even if the unfolding is reversible, since deuterium uptake is effectively irreversible in a large excess of D₂O. Under physiological conditions and in the absence of denaturant, such slow cooperative unfolding is rarely observed because the time scale of unfolding/refolding is generally much faster than the intrinsic rate of H/D exchange. However, it has been observed in some cases, most notably in certain SH3 domains (32).

We have observed this pattern of slow cooperative unfolding in residues 232–246 of p66, which is located at the base of the thumb subdomain and corresponds to β -strands 13 and 14 and a loop. Figure 7A shows the spectra of this peptide at 5, 10, 20, and 30 s of incubation in D₂O. The 5–30 s spectra show a double

Table 1: Comparison of the Number of Slow Exchanging Amide Hydrogens^a with the Number of Hydrogen Bonds^b

sequence	residue no.	p66 subunit			p51 subunit		
		n-slow	n-Whatif	ratio ^c	n-slow	n-Whatif	ratio ^c
MEKEGKISKIGPENPYNTPVF	41–61	11	14	0.79	11	13	0.85
WEVQLGIPHPAGLKKKSVTVL	88–109	7	10	0.70	8	10	0.80
DVGDAY	110–115	2	3	0.67	3	5	0.60
SVPLDEDF	117–124	4	4	1.00	3	3	1.00
FRKYTAFTIPSINNETPGIRYQY	124–146	13	12	1.08	13	16	0.81
NVLPQGWKGSPIAF	147–160	7	7	1.00	5	8	0.63
YMDDL	183–187	4	2	2.00	3	2	1.50
LYVGSD	187–192	5	4	1.25	5	4	1.25
LEIGQHRTKIEELRQHL	193–209	11	13	0.85	12	11	1.09
LRWGLTTPDKKHQKEPFLWMG	210–231	5	11	0.45	4	5	0.80
YELHPDKWTVQPIVL	232–246	3	7	0.43	0	3	0.00
PEKDSWTVND	247–256	3	4	0.75	4	5	0.80
IQKLVGKLNWASQIYPGIKVRQLCKL	257–282	13	20	0.65	7	18	0.39
LRGTKALTEVIPLTEEA	283–300	3	9	0.33	5	8	0.63
LELAENREILKEPVHGVYYDPSKDLIAE	301–328	10	20	0.50	11	17	0.65
IQKQGQGWYQ	329–340	5	8	0.63	6	9	0.67
IYQEPFKNLKTGKYARMGAHTNDVKQLTE	341–370	11	14	0.79	14	19	0.74
AVQKITTES	371–379	8	8	1.00	8	8	1.00
IVIWGKTPKFKLPIQKETWETW	380–401	12	15	0.80	13	16	0.81
VNTPPLVKL	417–425	1	2	0.50	0	3	0.00
WYQLEKEPIVGAET	426–439	2	2	1.00			
WYQLEKEPIVGAETF	426–440				2	1	2.00
LTNTTNQKTEL	469–479	2	6	0.33			
EVNIVTDSQ	492–500	8	6	1.33			
YALGIIQAQPDKSESEL	501–517	3	12	0.25			
VNQIIEQLIKKEKVYL	518–533	0	13	0.00			
AWVPAHKGIGGNEQVDKLVSAIRKIL	534–560	4	11	0.36			

^a Number of slow exchanging amide hydrogens taken from Supporting Information Tables S1 and S2. ^b Number of hydrogen bonds determined by WhatIf using the RT structure 1DLO. ^c Ratio of slow exchanging hydrogens to the number of hydrogen bonds.

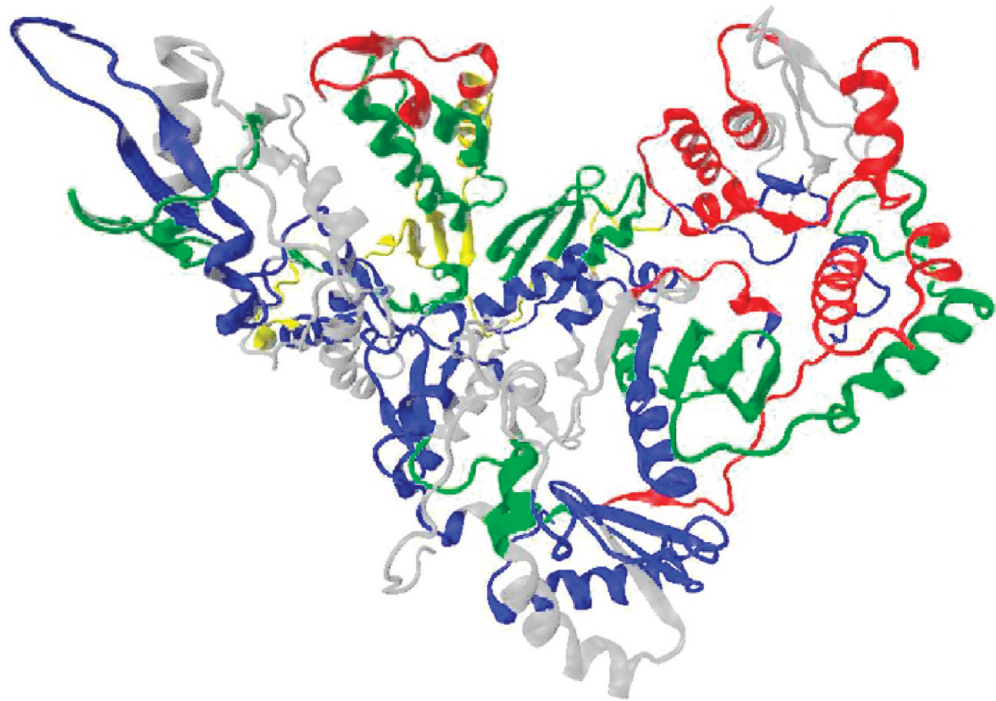


FIGURE 6: Stability of hydrogen bonds in RT. Structure of HIV-1 RT colored by the ratio of slow exchanging to hydrogen-bonded amide hydrogens: missing coverage (gray), very flexible regions (red, <0.4), flexible regions (yellow, 0.4–0.6), rigid regions (green, 0.6–0.8), and very rigid regions (blue, >0.8).

isotopic envelope as well as the disappearance of the lower m/z peak over time. Quantifying the relative amounts of folded and unfolded forms from the areas under Gaussian peaks indicates that the folded form disappears with a $t_{1/2} = 6.6$ s (Figure 7B).

Because the isotopic envelopes are not well resolved, the fitting to two Gaussian distributions is uncertain. Therefore, we also employed peak width analysis (33). Depending on the height at which peak widths were determined, a $t_{1/2} \sim 15$ –20 s for

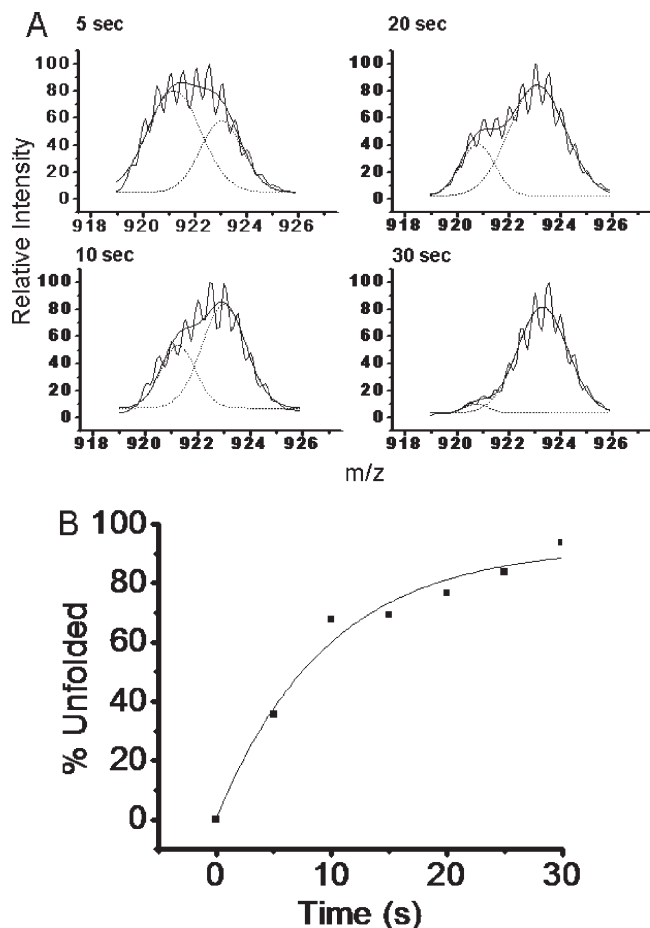


FIGURE 7: (A) Mass spectra of peptide 232–246 at different incubation times in RT buffer D–D₂O. The high and low m/z peaks are fit to Gaussian distributions (dotted lines). (B) Fraction unfolded as a function of time. Solid line is fit to a single exponential.

unfolding is obtained. This is approximately 2-fold larger than the value determined for Gaussian fitting.

DISCUSSION

Comparing the distribution of slow exchanging amide hydrogens with the distribution of hydrogen bonds indicates that the majority of secondary structural elements seen in the crystal structure of RT are relatively stable in solution (Figure 6). A major exception is the RNase H domain and the p51 thumb. Both of these regions exchange far more quickly than the crystal structure of RT or the solution structure of the isolated RNase H domain suggests. This high degree of conformational flexibility may allow the RNase H domain to reorient itself to accommodate different template/primer substrates and binding orientations (34). The isolated domain is well structured on the NMR time scale, except for 24 residues at the C-terminus (17). The absence of resonances for most of the C-terminal helix $\alpha E'$, which is present in the crystal structure of the isolated domain (35), is indicative of a slow conformational exchange process. The HXMS time scale (seconds to hours) is much slower than the NMR time scale (milliseconds to picoseconds). The fast exchanging amide hydrogens in peptide 534–560 of p66 observed by H/D exchange are consistent with an unstable C-terminus of the RNase H domain. In addition, the p66 thumb, while stable at short labeling times, shows substantial flexibility at longer times (Figure 5). This flexibility may allow for structural adaptation of

thumb subdomain residues to binding sites on the template/primer during polymerization.

Much of our current knowledge regarding the structural dynamics of RT comes from simulations. Bahar et al. (7) employed a coarse-grained approach called GNM to examine the global dynamics of RT. They found that the lowest frequency modes were dominated by motions of the fingers and thumb subdomains and RNase H domain of p66, whereas p51 was essentially rigid. While whole domain motions will not necessarily be reflected in H/D exchange rates, it is nonetheless instructive to compare our results with the results of a recent ANM analysis (36). The two approaches are in agreement that the palm and connection subdomains are relatively rigid and that the RNase H domain and p66 thumb domain are flexible (Figure 6C). In particular, the p51 thumb–RNase H interface shows little protection from exchange, indicating weak contacts between the two domains. The weakness of these contacts might facilitate the large-scale RNase H domain motions that are apparent in the lowest frequency normal modes.

The β -sheet $\beta 12$ – $\beta 13$ – $\beta 14$ lies at the base of the p66 thumb subdomain. It contains the highly conserved WMG loop that forms part of the primer grip, as well as residues F227, W229, and L234 that form part of the NNRTI binding pocket. The sheet is characterized as a hinge-bending center in the GNM analysis of the RT–nevirapine complex (7). The slow cooperative unfolding in peptide 232–246 indicates that this β -sheet is not stable in solution but is disrupted in a concerted manner, with an unfolding $t_{1/2}$ between 7 and 20 s. The p66 thumb subdomain assumes somewhat different orientations in different crystal structures. In the template/primer-bound structures it adopts an “open” conformation (4, 25, 26), in contrast to the “closed” conformation seen in the unliganded structures (5, 6). Of the RT–template/primer structures currently available, three show disruption of either β -strand 12 or 14 (25, 26, 37–41). On the basis of these observations, we suggest that the instability seen in β -strands 12, 13, and 14 may facilitate thumb subdomain motions.

Both analysis of viral genomes isolated from patients and directed mutagenesis studies have provided extensive information on the degree to which different regions of RT tolerate sequence variation. Ceccherini-Silberstein et al. (42) examined patterns of sequence variation in the first 320 residues of RT isolated from 1704 HIV-positive individuals and identified several contiguous stretches of high sequence conservation. Our H/D exchange experiments provide substantial sequence coverage for six of the nine regions. Of these six regions (residues 91–97, 107–117, 124–135, 147–157, 181–94, and 216–244), five are located in regions of rigid/stable structure, as evidenced by their relatively slow rates of H/D exchange. This is consistent with the general observation that proteins are less tolerant to mutations in regions that are tightly packed and/or involved in strong intramolecular interactions. The exception is the region defined by residues 216–244, which shows very rapid H/D exchange and contains β -sheet $\beta 12$ – $\beta 13$ – $\beta 14$ mentioned above. Ceccherini-Silberstein et al. (42) analyzed RT sequences from both drug-naïve and drug-treated patients and compared patterns of sequence conservation in the two populations. The stretch of residues 216–244 is one of three regions that are not conserved in drug-treated patients despite their high conservation in naïve patients. Two peptides, which together include residues 209–246, comprise the largest contiguous stretch of fast exchanging residues in the polymerase domain of RT and also

contain a number of mutations associated with drug resistance, K219, P225, F227, and K238.

ACKNOWLEDGMENT

The authors are grateful to Valerie A. Braz for discussion of HXMS data.

SUPPORTING INFORMATION AVAILABLE

Exchange rates for the p66 (Table S1) and p51 (Table S2) subunits and Figure S1 showing subunit separation. This material is available free of charge via the Internet at <http://pubs.acs.org>.

REFERENCES

- Coffin, J. M., Hughes, S. H., and Varmus, H. E. (1997) Retroviruses, Cold Spring Harbor Laboratory Press, Plainview, NY.
- Wang, J., Smerdon, S. J., Jäger, J., Kohlstaedt, L. A., Rice, P. A., Friedman, J. M., and Steitz, T. A. (1994) Structural basis of asymmetry in the human immunodeficiency virus type 1 reverse transcriptase heterodimer. *Proc. Natl. Acad. Sci. U.S.A.* 91, 7242–7246.
- Le Grice, S. F. J., Naas, T., Wohlgensinger, B., and Schatz, O. (1991) Subunit-selective mutagenesis indicates minimal polymerase activity in heterodimer-associated p51 HIV-1 reverse transcriptase. *EMBO J.* 10, 3905–3911.
- Jacobo-Molina, A., Ding, J., Nanni, R. G., Clark, A. D., Jr., Lu, X., Tantillo, C., Williams, R. L., Kamer, G., Ferris, A. L., Clark, P., Hizi, A., Hughes, S. H., and Arnold, E. (1993) Crystal structure of human immunodeficiency virus type 1 reverse transcriptase complexed with double-stranded DNA at 3.0 Å resolution shows bent DNA. *Proc. Natl. Acad. Sci. U.S.A.* 90, 6320–6324.
- Hsiou, Y., Ding, J., Das, K., Clark, A. D., Jr., Hughes, S. H., and Arnold, E. (1996) Structure of unliganded HIV-1 reverse transcriptase at 2.7 Å resolution: implications of conformational changes for polymerization and inhibition mechanisms. *Structure* 4, 853–860.
- Rodgers, D. W., Gambelin, S. J., Harris, B. A., Ray, S., Culp, J. S., Hellmig, B., Woolf, D. J., Debouck, C., and Harrison, S. C. (1995) The structure of unliganded reverse transcriptase from the human immunodeficiency virus type 1. *Proc. Natl. Acad. Sci. U.S.A.* 92, 1222–1226.
- Bahar, I., Erman, B., Jernigan, R. L., Atilgan, A. R., and Covell, D. G. (1999) Collective motions in HIV-1 reverse transcriptase: examination of flexibility and enzyme function. *J. Mol. Biol.* 285, 1023–1037.
- Madrid, M., Jacobo-Molina, A., Ding, J., and Arnold, E. (1999) Major subdomain rearrangement in HIV-1 reverse transcriptase simulated by molecular dynamics. *Proteins* 35, 332–337.
- Madrid, M., Lukin, J. A., Madura, J. D., Ding, J., and Arnold, E. (2001) Molecular dynamics of HIV-1 reverse transcriptase indicates increased flexibility upon DNA binding. *Proteins* 45, 176–182.
- Shen, L., Shen, J., Luo, X., Cheng, F., Xu, Y., Chen, K., Arnold, E., Ding, J., and Jiang, H. (2003) Steered molecular dynamics simulation on the binding of NNRTI to HIV-1 RT. *Biophys. J.* 84, 3547–3563.
- Carvalho, A. T. P., Fernandes, P. A., and Ramos, M. J. (2007) The excision mechanism in reverse transcriptase: pyrophosphate leaving and fingers opening are uncoupled events with the analogues AZT and d4T. *J. Phys. Chem. B* 111, 12032–12039.
- Rodríguez-Barrios, F., Perez, C., Lobaton, E., Velazquez, S., Chamorro, C., San-Felix, A., Perez-Perez, M. J., Camarasa, M. J., Pelemans, H., Balzarini, J., and Gago, F. (2001) Identification of a putative binding site for [2',5'-bis-(*tert*-butyldimethylsilyl)- β -D-ribofuranosyl]-3'-spiro-5''-(4''-amino-1'',2''-oxathiole-2'',2''-dioxide)thymine (TSAO) derivatives at the p51-p66 interface of HIV-1 reverse transcriptase. *J. Med. Chem.* 44, 1853–1865.
- Rodríguez-Barrios, F., Balzarini, J., and Gago, F. (2005) The molecular basis of resilience to the effect of the Lys103Asn mutation in non-nucleoside HIV-1 reverse transcriptase inhibitors studied by targeted molecular dynamics simulations. *J. Am. Chem. Soc.* 127, 7570–7578.
- Zhou, Z., Madrid, M., Evansek, J. D., and Madura, J. D. (2005) Effect of a bound non-nucleoside RT inhibitor on the dynamics of wild-type and mutant HIV-1 reverse transcriptase. *J. Am. Chem. Soc.* 127, 17253–17260.
- Kensch, O., Restle, T., Wohrl, B. M., Goody, R. S., and Steinhoff, H. J. (2000) Temperature-dependent equilibrium between the open and closed conformation of the p66 subunit of HIV-1 reverse transcriptase revealed by site-directed spin labelling. *J. Mol. Biol.* 301, 1029–1039.
- Powers, R., Clore, G. M., Stahl, S. J., Wingfield, P. T., and Gronenborn, A. (1992) Analysis of the backbone dynamics of the ribonuclease H domain of the human immunodeficiency virus reverse transcriptase using ^{15}N relaxation measurements. *Biochemistry* 31, 9150–9157.
- Pari, K., Mueller, G. A., DeRose, E. F., Kirby, T. W., and London, R. E. (2003) Solution structure of the RNase H domain of the HIV-1 reverse transcriptase in the presence of magnesium. *Biochemistry* 42, 639–650.
- Mueller, G. A., Pari, K., DeRose, E. F., Kirby, T. W., and London, R. E. (2004) Backbone dynamics of the RNase H domain of HIV-1 reverse transcriptase. *Biochemistry* 43, 9332–9342.
- Wales, T. E., and Engen, J. R. (2006) Hydrogen exchange mass spectrometry for the analysis of protein dynamics. *Mass Spectrom. Rev.* 25, 158–170.
- Le Grice, S. F. J., Cameron, C. E., and Benkovic, S. J. (1995) Purification and characterization of human immunodeficiency virus type 1 reverse transcriptase. *Methods Enzymol.* 262, 130–144.
- Venezia, C. F., Howard, K. J., Ignatov, M. E., Holladay, L. A., and Barkley, M. D. (2006) Effects of efavirenz binding on the subunit equilibria of HIV-1 reverse transcriptase. *Biochemistry* 45, 2779–2789.
- Tsutsui, Y., Liu, L., Gershenson, A., and Wintrobe, P. L. (2006) The conformational dynamics of a metastable serpin studied by hydrogen exchange and mass spectrometry. *Biochemistry* 45, 6561–6569.
- Divita, G., Ritinger, K., Restle, T., Immendorfer, U., and Goody, R. S. (1995) Conformational stability of dimeric HIV-1 and HIV-2 reverse transcriptases. *Biochemistry* 34, 16337–16346.
- Zhang, Z., and Smith, D. L. (1993) Determination of amide hydrogen exchange by mass spectrometry: a new tool for protein structure elucidation. *Protein Sci.* 2, 522–531.
- Huang, H., Chopra, R., Verdine, G. L., and Harrison, S. C. (1998) Structure of a covalently trapped catalytic complex of HIV-1 reverse transcriptase: implications for drug resistance. *Science* 282, 1669–1675.
- Sarafianos, S. G., Das, K., Tantillo, C., Clark, A. D., Jr., Ding, J., Whitcomb, J. M., Boyer, P. L., Hughes, S. H., and Arnold, E. (2001) Crystal structure of HIV-1 reverse transcriptase in complex with a polypurine tract RNA:DNA. *EMBO J.* 20, 1449–1461.
- Das, K., Lewi, P. J., Hughes, S. H., and Arnold, E. (2005) Crystallography and the design of anti-AIDS drugs: conformational flexibility and positional adaptability are important in the design of non-nucleoside HIV-1 reverse transcriptase inhibitors. *Prog. Biophys. Mol. Biol.* 88, 209–231.
- Englander, S. W., and Kallenbach, N. R. (1983) Hydrogen exchange and structural dynamics of proteins and nucleic acids. *Q. Rev. Biophys.* 16, 521–655.
- Jacques, P. S., Wohrl, B. M., Howard, K. J., and Le Grice, S. F. J. (1994) Modulation of HIV-1 reverse transcriptase function in “selectively deleted” p66/p51 heterodimers. *J. Biol. Chem.* 269, 1388–1393.
- Hooft, R. W., Sander, C., and Vriend, G. (1996) Positioning hydrogen atoms by optimizing hydrogen-bond networks in protein structures. *Proteins* 26, 363–376.
- Deng, Y., and Smith, D. L. (1999) Rate and equilibrium constants for protein unfolding and refolding determined by hydrogen exchange-mass spectrometry. *Anal. Biochem.* 276, 150–160.
- Engen, J. R., Smithgall, T. E., Gmeiner, W. H., and Smith, D. L. (1997) Identification and localization of slow, natural, cooperative unfolding in the hematopoietic cell kinase SH3 domain by amide hydrogen exchange and mass spectrometry. *Biochemistry* 36, 14384–14391.
- Weis, D. D., Wales, T. E., Engen, J. R., Hotchkiss, M., and Ten Eyck, L. F. (2006) Identification and characterization of EX1 kinetics in H/D exchange mass spectrometry by peak width analysis. *J. Am. Soc. Mass Spectrom.* 17, 1498–1509.
- Abbondanzieri, E. A., Bokinsky, G., Rausch, J. W., Zhang, J. X., Le Grice, S. F. J., and Zhuang, X. (2008) Dynamic binding orientations direct activity of HIV reverse transcriptase. *Nature* 453, 184–189.
- Davies, J. F., II, Hostomska, Z., Hostomsky, Z., Jordan, S. R., and Matthews, D. A. (1991) Crystal structure of the ribonuclease H domain of HIV-1 reverse transcriptase. *Science* 252, 88–95.
- Bahar, I. (2009) Anisotropic Network Model web server, <http://ignmtest.cccb.pitt.edu/cgi-bin/anm/anm1.cgi>.
- Jaeger, J., Restle, T., and Steitz, T. A. (1998) The structure of HIV-1 reverse transcriptase complexed with an RNA pseudoknot inhibitor. *EMBO J.* 17, 4535–4542.
- Sarafianos, S. G., Das, K., Clark, A. D., Jr., Ding, J., Boyer, P. L., Hughes, S. H., and Arnold, E. (1999) Lamivudine (3TC) resistance in HIV-1 reverse transcriptase involves steric hindrance with β -branched amino acids. *Proc. Natl. Acad. Sci. U.S.A.* 96, 10027–10032.

39. Sarafianos, S. G., Clark, A. D., Jr., Das, K., Tuske, S., Birktoft, J. J., Ilankumaran, P., Ramesha, A. R., Sayer, J. M., Jerina, D. M., Boyer, P. L., Hughes, S. H., and Arnold, E. (2002) Structures of HIV-1 reverse transcriptase with pre- and post-translocation AZTMP-terminated DNA. *EMBO J.* 21, 6614–6624.
40. Peletskaya, E. N., Kogon, A. A., Tuske, S., Arnold, E., and Hughes, S. H. (2004) Nonnucleoside inhibitor binding affects the interactions of the fingers subdomain of human immunodeficiency virus type 1 reverse transcriptase with DNA. *J. Virol.* 78, 3387–3397.
41. Tuske, S., Sarafianos, S. G., Clark, A. D., Jr., Ding, J., Naeger, L. K., White, K. L., Miller, M. D., Gibbs, C. S., Boyer, P. L., Clark, P., Wang, G., Gaffney, B. L., Jones, R. A., Jerina, D. M., Hughes, S. H., and Arnold, E. (2004) Structures of HIV-1 RT-DNA complexes before and after incorporation of the anti-AIDS drug tenofovir. *Nat. Struct. Mol. Biol.* 11, 469–474.
42. Ceccherini-Silberstein, F., Gago, F., Santoro, M., Gori, C., Svicher, V., Rodriguez-Barrios, F., d'Arrigo, R., Ciccozzi, M., Bertoli, A., d'Arminio Monforte, A., Balzarini, J., Antinori, A., and Perno, C. F. (2005) High sequence conservation of human immunodeficiency virus type 1 reverse transcriptase under drug pressure despite the continuous appearance of mutations. *J. Virol.* 79, 10718–10729.